European Journal of Pharmacology 955 (2023) 175928

Contents lists available at ScienceDirect

European Journal of Pharmacology

journal homepage: www.elsevier.com/locate/ejphar

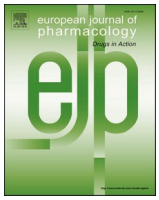

Sodium hydrosulfide moderately alleviates the hallmark symptoms of Duchenne muscular dystrophy in *mdx* mice

Małgorzata Myszka [a,b], Olga Mucha [a], Paulina Podkalicka [a], Urszula Waśniowska [a], Józef Dulak [a], Agnieszka Łoboda [a,*]

[a] Department of Medical Biotechnology, Faculty of Biochemistry, Biophysics and Biotechnology, Jagiellonian University, Gronostajowa 7, Kraków, 30-387, Poland
[b] Doctoral School of Exact and Natural Sciences, Jagiellonian University, Prof. St. Łojasiewicz 11, 30-348, Krakow, Poland

ARTICLE INFO

Keywords:
DMD
Duchenne muscular dystrophy
Hydrogen sulfide
NaHS
Sodium hydrosulfide
mdx

ABSTRACT

Duchenne muscular dystrophy (DMD) is an incurable disease caused by mutations in the X-linked DMD gene that encodes a structural muscle protein, dystrophin. This, in turn, leads to progressive degeneration of the skeletal muscles and the heart. Hydrogen sulfide (H_2S), the pleiotropic agent with antioxidant, anti-inflammatory, and pro-angiogenic activities, could be considered a promising therapeutic factor for DMD.

In this work, we studied the effect of daily intraperitoneal administration of the H_2S donor, sodium hydrosulfide (NaHS, 100 μmol/kg/day for 5 weeks) on skeletal muscle (gastrocnemius, diaphragm and tibialis anterior) pathology in dystrophin-deficient *mdx* mice, characterized by decreased expression of H_2S-generating enzymes.

NaHS reduced the level of muscle damage markers in plasma (creatine kinase, lactate dehydrogenase and osteopontin). It lowered oxidative stress by affecting the GSH/GSSG ratio, up-regulating the level of cytoprotective heme oxygenase-1 (HO-1) and down-regulating the NF-κB pathway. In the gastrocnemius muscle, it also increased angiogenic vascular endothelial growth factor (*Vegf*) and its receptor (*Kdr*) expression, accompanied by the elevated number of α-SMA/CD31/lectin-positive blood vessels. The expression of fibrotic regulators, like *Tgfβ*, *Col1a1* and *Fn1* was decreased by NaHS in the tibialis anterior, while the level of autophagy markers (AMPKα signalling and *Atg* genes), was mostly affected in the gastrocnemius. Histological and molecular analysis showed no effect of H_2S donor on regeneration and the muscle fiber type composition.

Overall, the H_2S donor modified the gene expression and protein level of molecules associated with the pathophysiology of DMD, contributing to the regulation of oxidative stress, inflammation, autophagy, and angiogenesis.

1. Introduction

Duchenne muscular dystrophy (DMD) is caused by the lack of dystrophin, the muscle functional protein, due to over 7000 patient-specific mutations in one of the largest human genes, *DMD* (Bladen et al., 2015; Carter et al., 2018). This devastating progressive disease of the skeletal and respiratory muscles, as well as the heart, is still incurable. Consequently, new therapeutic options remain the unmet need in DMD.

The pivotal role of dystrophin is to provide mechanical stabilization and integrity of the muscle membrane during force generation (Gao and McNally, 2015). The absence of functional dystrophin has detrimental effects on muscle function, including increased inflammation, fibrosis, and oxidative stress (Hoffman et al., 1987). Impaired autophagy and angiogenesis have also been suggested to be hallmarks of DMD (De Palma et al., 2014; Podkalicka et al., 2019). In patients, early signs of motor impairment manifest between the ages of 2 and 5 years, while rapid progression of the disease occurs between the ages of 10–14. Later, patients begin to suffer from respiratory and cardiac failure that leads to death around the second or third decades of life (Emery, 2002).

To study DMD, mouse models are frequently used; however, they do not fully resemble human pathology. The mouse *mdx* model, which has the spontaneous mutation in exon 23 of the *Dmd* gene that results in the loss of the dystrophin expression (Bulfield et al., 1984; Sicinski et al., 1989), varies in the course of the disease and presents a mild phenotype with normal lifespan, when compared to human DMD patients. It is also well known that because of variance in general metabolism and, for

* Corresponding author.
E-mail address: agnieszka.loboda@uj.edu.pl (A. Łoboda).

https://doi.org/10.1016/j.ejphar.2023.175928
Received 22 November 2022; Received in revised form 22 June 2023; Accepted 18 July 2023
Available online 26 July 2023

example, the proportion of slow and fast twitch fibers, the hallmarks of DMD may be accelerated in specific muscles. Therefore, the effect of possible modulators of DMD progression can be exerted in a muscle-dependent way.

Although some mutation-specific drugs (eteplirsen, golodirsen, viltolarsen, casimersen and ataluren), which restore functional dystrophin expression, have recently been revealed, they are suitable only for small subpopulations of affected individuals and their efficacy has not yet been fully proven (Birnkrant et al., 2018; Dulak, 2021). On the other hand, glucocorticoids (GCs), a gold standard therapy for DMD patients, act primarily as anti-inflammatory agents by inhibiting the signalling of the nuclear factor kappa-light-chain-enhancer of activated B cells (NF-κB) and exert many adverse effects that lead, among others, to osteoporosis, diabetes, and muscle atrophy (Schäcke et al., 2002).

Recently, our group has demonstrated that genetic or chemical inhibition of heme oxygenase-1 (HO-1), an enzyme with cytoprotective, pro-angiogenic, and anti-inflammatory properties, profoundly exacerbated the dystrophic phenotype (Pietraszek-Gremplewicz et al., 2018). Given that HO-1 and its product, CO, may share effects similar to hydrogen sulfide (H_2S) (Giuffrè and Vicente, 2018), our objective was to check the effect of this gaseous mediator in the mouse model of DMD.

H_2S, generated by endogenous enzymes, mainly cystathionine γ-lyase (CTH, CGL or CSE), cystathionine β-synthase (CBS), and 3-mercaptopyruvate sulfurtransferase (MPST or 3-MST) can exert antioxidant, antifibrotic, antiapoptotic and anti-inflammatory activities. Other known effects are related to neuroprotection and regulation of angiogenesis (Giuffrè and Vicente, 2018; Podkalicka et al., 2022). Therefore, H_2S therapy can be postulated to mitigate the progression of DMD by attenuating oxidative stress, inflammation, and fibrosis.

We have found that daily intraperitoneal administration of the fast-releasing H_2S donor, sodium hydrosulfide (NaHS, 100 μmol/kg body weight for 5 weeks), regulates the expression of genes and proteins involved in the progression of DMD, including inflammation, oxidative stress, fibrosis, angiogenesis, and autophagy, but these effects could be muscle-specific. Interestingly, although NaHS decreased the level of osteopontin, the dystrophic-induced muscle damage marker and increased cytoprotective HO-1 level in the gastrocnemius, diaphragm and tibialis anterior muscles, the angiogenic and fibrotic regulators were affected in a muscle-dependent manner. We believe that this gaseous mediator has the potential to alleviate the hallmark symptoms of DMD.

2. Materials and methods

2.1. Animals

All animal work was performed following Animal Research: Reporting of In Vivo Experiments (ARRIVE) guidelines and regulations. The experiments were approved by the 2nd Institutional Animal Care and Use Committee (IACUC) in Kraków, Poland (approval number 261/2020). Wild-type (WT, C57BL/10ScSnJ) and *mdx* (C57BL/10ScSn-*Dmd*^{mdx}/J) mice were purchased from Jackson Laboratory (Bar Harbor, ME, USA, stock nos. 000476 and 001801, respectively). Mice were housed under specific pathogen-free (SPF) conditions in individually ventilated cages with a 14 h/10 h light/dark cycle and were kept on a normal, chow diet with water and food available *ad libitum*. Animal genotyping was performed using PCR on DNA isolated from tails.

2.2. Treatment with H_2S donor

NaHS treatment was initiated in 5-6-week-old animals. For 5 weeks, *mdx* mice received 100 μmol/kg body weight (BW) NaHS or solvent (NaCl) daily by intraperitoneal injection. WT animals that received a vehicle were used as a reference group. The dose of NaHS was chosen based on the literature data (Gomez et al., 2019; Ng et al., 2017; Yu et al., 2015). At the end of the experiment, muscles (gastrocnemius, tibialis anterior and diaphragm) and blood were collected for further analyses.

2.3. Grip strength assay

To assess the limb strength of *mdx* mice, a grip strength meter with a triangular pull bar (Ugo Basile) was used by the investigator blind to the mice's genotype. The test was performed one day after the last dose of NaHS administration as previously described (Aartsma-Rus and van Putten, 2014; Bronisz-Budzyńska et al., 2020; Mucha et al., 2021b) and following the instruction described in the TREAT-NMD SOP (https://treat-nmd.org/wp-content/uploads/2016/08/MDX-DMD_M.2.2.001.pdf). The measurements were repeated 4 times with a 1 min break between. The results were calculated as an average of all measurements, normalized to body weight (BW) and expressed as N/kg BW.

2.4. Blood cell count

Hematological parameters, including the total number of white blood cells (WBC) and the percentage of granulocytes, monocytes, and lymphocytes among WBC, were measured using EDTA-anticoagulated blood with scil Vet abc hematology analyser (Horiba ABX).

2.5. RNA isolation, reverse transcription (RT), and quantitative real-time PCR (qRT-PCR)

Total RNA was isolated using the Chomczynski-Sacchi method (Chomczynski and Sacchi, 1987). Briefly, at the end of the experiment, muscles were excised to RNAlater Stabilization Solution (Millipore Sigma/Sigma-Aldrich), snap-frozen in liquid nitrogen, and stored at −80 °C for downstream analyses. After determination of its quality and concentration with a NanoDrop Spectrophotometer (Thermo Fisher Scientific), 1000 ng of RNA was transcribed by recombinant M-MuLV reverse transcriptase (Thermo Fisher Scientific) into cDNA according to our previously published protocol (Pietraszek-Gremplewicz et al., 2018). qRT-PCR was performed on obtained cDNA with SYBR Green PCR Master Mix (Millipore Sigma/Sigma-Aldrich), and specific primers (listed in Table 1). *Eef2* was used as a housekeeping gene. The relative quantification of gene expression was calculated based on the

Table 1
Sequences of primers used for the determination of gene expression by qRT-PCR.

Gene	*Sequence 5'-3'*
Atg5	*F: CTGAAGATGGAGAGAAGAGG*
	R: GGGGACAATGCTAATATGAAG
Atg7	*F: CTGTTCACCCAAAGTTCTTG*
	R: TCTAAGAAGGAATGTGAGGAG
Cbs	*F: CCTAATTCTCACATTCTGGAC*
	R: GACACCGATGATTTTACAGC
Col1a1	*F: CGATCCAGTACTCTCCGCTCTTCC*
	R: ACTACCGGGCCGATGATGCTAACG
Cth	*F: GAAAAGGTTGTTTATCCTGGG*
	R: CTTGATGTAGAAACTGACCATC
Eef2	*F: AGAACATATTATTGCTGGCG*
	R: AACAGGGTCAGATTTCTTG
Il-6	*F: TACCACTTCACAAGTCGGAGGC*
	R: CTGCAAGTGCATCATCGTTGTTC
Kdr	*F: CGGCCAAGTGATTGAGGCAG*
	R: ATGAGGGCTCGATGCTCGCT
Mpst	*F: CGTCCTACTTGCTTTTCTC*
	R: CAGAGCTCGGAAAAGTTG
Myh3	*F:* TCTAGCCGGATGGTGGTCC
	R: GAATTGTCAGGAGCCACGAA
Spp1	*F: CCATCTCAGAAGCAGAATCTCCTT*
	R: GGTCATGGCTTTCATTGGAATT
Tgfb1	*F: GGATACCAACTATTGCTTGAG*
	R: TGTCCAGGCTCCAAATATAG
Vegfa	*F: ATGCGGATCAAACCTCACCAA*
	R: TTAACTCAAGCTGCCTCGCCT

comparative cycle threshold (C_t) method (according to the $2^{-\Delta Ct}$ formula where $\Delta C_t = C_{t\ \text{gene of interest}} - C_{t\ Eef2}$).

2.6. Western blotting

Total protein was isolated from snap-frozen muscles by homogenization in lysis buffer (ice-cold PBS containing proteinase inhibitors (Roche Diagnostic) and 1% Triton X100 (BioShop) using TissueLyser (Qiagen). Protein concentration was determined by bicinchoninic assay (BCA; Sigma-Aldrich) and 20 μg of protein lysate was processed as previously described (Pietraszek-Gremplewicz et al., 2018). If needed, the membranes were cut before the incubation with the following antibodies at the specified dilution: (i) primary antibodies - rabbit polyclonal anti–CTH (ab151769, Abcam, 1:1000), rabbit polyclonal anti–CBS (14787-1-AP, Proteintech, 1:1000), rabbit polyclonal anti–MPST (HPA001240, Sigma–Aldrich, 1:500), rabbit polyclonal anti–HO-1 (ADI-SPA-894, Enzo Life Sciences, 1:500), , rabbit polyclonal anti–AMPKα (2603 S, Cell Signalling Technology, 1:1000), rabbit polyclonal anti–phospho-AMPKα (2535, Cell Signalling Technology, 1:1000), rabbit monoclonal anti–NF-κB p65 (4764, Cell Signalling Technology, 1:1000), monoclonal mouse anti–phospho-IκBα (Ser32/36) (9246, Cell Signalling Technology, 1:1000), mouse monoclonal anti–vinculin (V9131, Sigma–Aldrich, 1:200), monoclonal mouse anti-GAPDH (60004-1-Ig, Proteintech, 1:1000) and (ii) secondary antibodies (conjugated with HRP) - anti-mouse IgG (554 002, BD Biosciences) for the detection of vinculin, GAPDH or phospho-IκBα (Ser32/36), as well as anti-rabbit IgG (7074, Cell Signaling Technology) for the detection of CTH, CBS, MPST, HO-1, AMPKα, phospho-AMPKα, and NF-κB p65. Membrane stripping was performed using 0.1 M glycine pH 2.6 (2 × 30 min incubation). Band densities of the target proteins were quantified using ImageJ software in relation to the vinculin or GAPDH level. The results of the densitometric analysis were normalized to the WT animals.

2.7. Determination of creatine kinase (CK) and lactate dehydrogenase (LDH) activity

Commercially available Liquick Cor-CK and Liquick Cor-LDH kits (Cormay) were used to assess CK and LDH activity, respectively, in 10-times diluted mouse plasma. After measurement, the absorbance values were converted to CK and LDH activity (U/l).

2.8. Enzyme-linked immunosorbent assay (ELISA)

The protein lysates were prepared from muscle fragments by homogenization in 1% Triton X-100 in PBS using TissueLyser (Qiagen), followed by centrifugation at 10 000 *g*, 10 min, 4 °C. The total protein concentration was measured by bicinchoninic acid assay (BCA, Sigma-Aldrich). 50 μg of protein lysate was used to determine the level of transforming growth factor-1 β (TGF-β) and 100 μg for fibroblast growth factor-2 (FGF2) according to the vendor's instructions (R&D Systems). The osteopontin (OPN) content was analysed in the gastrocnemius, tibialis anterior and diaphragm muscles and in 750 times-diluted mouse plasma and the concentration was quantified based on the absorbance values according to the manufacturer's protocol (R&D Systems). The concentration of HO-1 was evaluated using 50 μg of protein lysates with the Mouse Heme Oxygenase 1 SimpleStep ELISA Kit (Abcam).

2.9. Glutathione content

Protein lysates were prepared from muscle fragments by homogenization in 1% Triton X-100 in PBS using TissueLyser (Qiagen), followed by centrifugation at 10 000 *g*, 10 min, 4 °C. Total protein concentration was measured using a bicinchoninic acid assay (BCA, Sigma-Aldrich) and 150 μg of protein lysate was used to measure the reduced (GSH) and oxidized (GSSG) glutathione content using Glutathione Colorimetric Detection Kit according to the vendor's instruction (Invitrogen).

2.10. Hydroxyproline measurement

The colorimetric Hydroxyproline Assay Kit (MAK008, Sigma-Aldrich) was used to quantify the collagen content in lysates from muscle tissue fragments according to the manufacturer's protocol.

2.11. Histological and immunofluorescent analyses of muscles

For histological evaluation, muscles were collected and pre-treated with OCT medium (Leica) for a few minutes directly after collection. Subsequently, they were transferred to new OCT-containing tubes, frozen in liquid nitrogen-cooled isopentane, and stored at −80 °C. Then, 10 μm thick sections were cut on a cryotome (Leica), placed on the poly-L-lysine coated slides, air-dried for at least 2 h, and kept at −20 °C for further analyses. Hematoxylin and eosin (H&E) staining and Masson's trichrome staining were performed using the 4% buffered formalin-fixed (pH 7.4) frozen sections. For H&E, tissue sections were incubated in Mayer's hematoxylin (Sigma-Aldrich) for 12 min, rinsed with tap water (15 min), and stained for 1.5 min in 0.1% eosin solution (96% EtOH and distilled water, 7:3) (Sigma-Aldrich). After staining, the sections were incubated in increasing concentrations (70%, 96% (× 2), 99.8% (× 2)) of aqueous EtOH (Avantor Performance Materials Poland S.A.), then 2 times in xylene (Sigma-Aldrich) and sealed in Histofluid medium (Chemilab). Masson's trichrome staining (Trichrome Stain (Masson) Kit, Sigma-Aldrich) was performed following the manufacturer's protocol. After staining, the sections were incubated in increasing concentrations (70%, 96% (× 2), 99.8% (× 2)) of aqueous EtOH, then 2 times in xylene and sealed in Histofluid medium. Analyses were conducted according to our previous studies (Bronisz-Budzyńska et al., 2019; Kozakowska et al., 2018; Pietraszek-Gremplewicz et al., 2018) after taking pictures of the whole tissues using a Nikon Eclipse microscope. The assessment of inflammation and fibrosis extent was conducted using arbitrary units, respectively: 0 – no signs of inflammation/collagen deposition; 1 – any sign of leukocyte infiltration and myofiber swelling/collagen deposition; 2 – visible inflammation, myofiber swelling, and rhabdomyolysis/collagen deposition; 3 – signs of inflammation, myofiber swelling, and rhabdomyolysis take around half of a field of view/collagen deposition takes up around half of the field of view; 4 – a substantial part of the muscle in the field of view is infiltrated and degenerated/collagen deposition takes the substantial part of the field of view. The analysis of centrally nucleated fibers (CNF) indicating the level of regeneration was performed based on H&E staining; 10–15 pictures/tissue sections were randomly taken and the percentage of CNF among all fibers was calculated.

Immunofluorescent staining of α-SMA/CD31/lectin and CD45 was performed on the gastrocnemius and tibialis frozen sections. After drying, sections were fixed in 10% formalin solution for 10 min and washed with PBS (2 × 3 min). For membrane permeabilization, 10 min incubation in 0.2% Triton X-100 in PBS was performed followed by washing once with PBS. Subsequently, sections were incubated for 40 min in 0.2% Sudan Black (Sigma-Aldrich) solution in 70% EtOH, then washed 3 times with PBS, followed by 1 h blocking in PBS solution with 10% goat serum (GS) and 1% bovine serum albumin (BSA). Overnight incubation with primary antibodies: rat-anti mouse CD31 (550 274, BD Bioscience, 1:150), rabbit-anti mouse α-smooth muscle actin (α-SMA, ab5694, Abcam 1:200), anti-lectin GSL I – B4 (DL-1208-5, Griffonia Simplicifolia Lectin I Isolectin B4, DyLight 649, 1:67) and rat-anti mouse CD45 (550 539, BD Bioscience, 1:200) diluted in PBS containing 1% GS, 0.1% BSA was performed in 4 °C. After washing with PBS (3 × 3 min), secondary antibodies including donkey anti-rabbit IgG Alexa Fluor 488 (A21206) for detection of α-SMA in green and goat anti-rat IgG Alexa Fluor 568 (A11077) for detection of CD31 and CD45 in red (all from Invitrogen, 1:500) with 0.2 μg/mL DAPI were added and incubated for 1 h in RT. After that, sections were washed with PBS (3 × 3 min) and mounted with

Daco fluorescent mounting medium. The negative control was prepared by omitting the primary antibodies in the procedure described above. Pictures were taken using Olympus IX83 microscope. Quantification of vessels positive for α-SMA/CD31/lectin and area positive for CD45 was performed using ImageJ software. Nicotinamide adenine dinucleotide dehydrogenase-tetrazolium reductase (NADH-TR) staining was performed to determine the extent of oxidative fibers in the whole muscle sections as in our previous study (Podkalicka et al., 2020). Briefly, sections were air dried for 15 min before the staining. Subsequently, the slides were transferred to the solution mixture prepared in 0.05 M TRIS buffer (pH 7.6) of 1:1 8 mg/5 mL (NADH) and 10 mg/5 mL nitro blue tetrazolium chloride (NBT) and incubated for 30 min at 37 °C. After that, the slides were washed with three exchanges of deionized water. The unbound staining was removed from the sections with three exchanges each of the 30%, 60%, 90%. acetone solutions in increasing and decreasing concentration. All reagents were purchased from Millipore Sigma/Sigma-Aldrich. Finally, the slides were rinsed several times in deionized water and mounted in an aqueous mounting medium Aquatex (Sigma-Aldrich). The staining was visualized under Leica DMi8 microscope. Analysis of the dark (oxidative) and pale (glycolytic) regions was performed using QuPath software. All histological and immunofluorescent assessments were analysed by the investigator blind to the mice group. If necessary, the brightness and/or contrast were adjusted to all of the pictures equally.

2.12. Statistical analyses

Data are presented as mean ± SEM. The differences between the groups were tested for statistical significance using the one-way ANOVA followed by Tukey's post-hoc test and, when indicated, the unpaired 2-tailed Student's *t*-test; $p \leq 0.05$ was considered significant. The statistically significant outliers were identified based on Grubbs' test and were excluded from the analysis. The *n* number indicating the number of animals per group, as well as the specific statistical test used, were included in the figure legend.

3. Results

3.1. NaHS treatment is well tolerated by dystrophic animals

It is well known that *mdx* mice, as well as patients with DMD, are characterized by muscle hypertrophy and the so-called pseudohypertrophy as the result of the accumulation of fat and connective tissue (Kornegay et al., 2012). Similarly to our previous observations (Podkalicka et al., 2020), in the present study, we have noticed an increase in body weight of *mdx* mice compared to their WT counterparts (Supplementary Fig. 1A). Daily treatment with NaHS (100 μmol/kg/day) for 5 weeks was well tolerated by dystrophic mice, as no loss of body weight was observed (Supplementary Fig. 1A). Furthermore, NaHS did not affect the count of WBC, lymphocytes, granulocytes, and monocytes (Supplementary Figs. 1B–E).

3.2. The expression of H_2S-generating enzymes is decreased in mdx mice

Analysis of the gastrocnemius muscle of dystrophin-deficient *mdx* mice showed a decrease in the gene expression of H_2S-generating enzymes such as cystathionine γ-lyase (*Cth*) (Fig. 1A), cystathionine β-synthase (*Cbs*) (Fig. 1B) and 3-mercaptopyruvate sulfurtransferase (*Mpst*) (Fig. 1C). The reduced protein level of all enzymes in dystrophic gastrocnemius was noted, as indicated by representative Western blot (Fig. 1D) and its densitometric quantification (Supplementary Figs. 2A–C). A similar drop in the CTH level was found in dystrophic diaphragm and tibialis anterior (Fig. 1E and F, Supplementary Figs. 2D and G); while the expression of CBS and MPST was decreased in the *mdx* diaphragm but not in the tibialis anterior (Fig. 1E–G, Supplementary Fig. 2E-F, H-I). NaHS restored *Cth* expression to the level of WT animals (Fig. 1A). However, the expression of *Cbs* and *Mpst* mRNA (Fig. 1B and C) was not regulated, similarly to the protein level of all H_2S-generating enzymes in three different muscles (except the CTH level in the diaphragm, which was slightly increased) (Fig. 1D–F, Supplementary Fig. 2).

3.3. The level of muscle damage markers and the ratio of GSH/GSSG are altered after treatment with the H_2S donor

To determine the impact of NaHS treatment on the hallmark symptoms of the disease, we measured the level of osteopontin, a biomarker of DMD (Kuraoka et al., 2016). We detected an increased expression of the transcript (*Spp1*) (Fig. 2A) and protein level (OPN) (Fig. 2B) in the gastrocnemius muscle with their concomitant down-regulation after NaHS administration. Similar effects were found in the diaphragm (Fig. 2C) and tibialis anterior (Fig. 2D) muscles. Additionally, the level of muscle damage indicators evaluated in plasma, OPN (Fig. 2E) and creatine kinase (CK) activity (Fig. 2F), increased markedly in *mdx* animals and decreased in NaHS-administered mice. Furthermore, the activity of lactate dehydrogenase (LDH), another blood-derived DMD marker, was diminished in *mdx* mice receiving NaHS compared to *mdx* mice (Fig. 2G).

H_2S has been implicated to exhibit antioxidant properties through regulation of glutathione production (Parsanathan and Jain, 2018). Consequently, we determined the ratio of reduced glutathione (GSH), the master antioxidant marker and the scavenger of reactive oxygen species (ROS), to its oxidized form (GSSG). We demonstrated a decrease in the GSH/GSSG ratio in *mdx* mice, while administration of NaHS to dystrophic animals restored it to the control level, confirming its antioxidant properties (Fig. 2H).

3.4. NaHS increases the expression of cytoprotective heme oxygenase-1

We have previously reported that heme oxygenase-1 (HO-1), a cytoprotective, anti-inflammatory and antioxidant enzyme, exerts a protective role in *mdx* animals (Pietraszek-Gremplewicz et al., 2018). In the current study, treatment with NaHS led to a significant increase in the level of the HO-1 protein in the gastrocnemius muscle (Fig. 3A), diaphragm (Fig. 3B), and tibialis anterior (Fig. 3C) as evaluated by ELISA. This effect was also confirmed by Western blotting, as shown by representative results with densitometric analysis in the gastrocnemius (Fig. 3D and E) and diaphragm (Fig. 3F and G).

3.5. Administration of NaHS inhibits the pro-inflammatory NF-κB signalling pathway

Dystrophic muscles are characterized by chronic inflammation (Rosenberg et al., 2015), and inhibitors of the NF-κB pathway, such as GCs, represent the gold standard treatment in DMD (Schäcke et al., 2002). NF-κB activation depends on phosphorylation that induces proteasomal degradation of the inhibitor of NF-κB proteins (IκBs) which retain inactive NF-κB dimers in the cytosol (Oeckinghaus and Ghosh, 2009). We demonstrated decreased protein expression of NF-κB and phosphorylation of IκB after treatment with the H_2S donor in the gastrocnemius (Fig. 4A–C), indicating anti-inflammatory properties of NaHS. Additionally, similar effects were observed when the expression of interleukin-6 (*Il-6*), one of the NF-κB-regulated cytokines was evaluated (Fig. 4D).

To check whether up-regulation of HO-1 and inhibition of the NF-κB pathway by NaHS affect global muscle inflammation, we performed hematoxylin and eosin (H&E) staining (Fig. 4E–G) and immunofluorescent staining of CD45, a pan-leukocyte marker (Fig. 4H–K). A calculation of the sections indicated a prominent inflammatory infiltration in gastrocnemius (Fig. 4E and F), tibialis anterior (Fig. 4G) and diaphragm (data not shown) and an increase in the area of CD45 + (Fig. 4H–K) in the dystrophic muscles; however, the H_2S donor was not

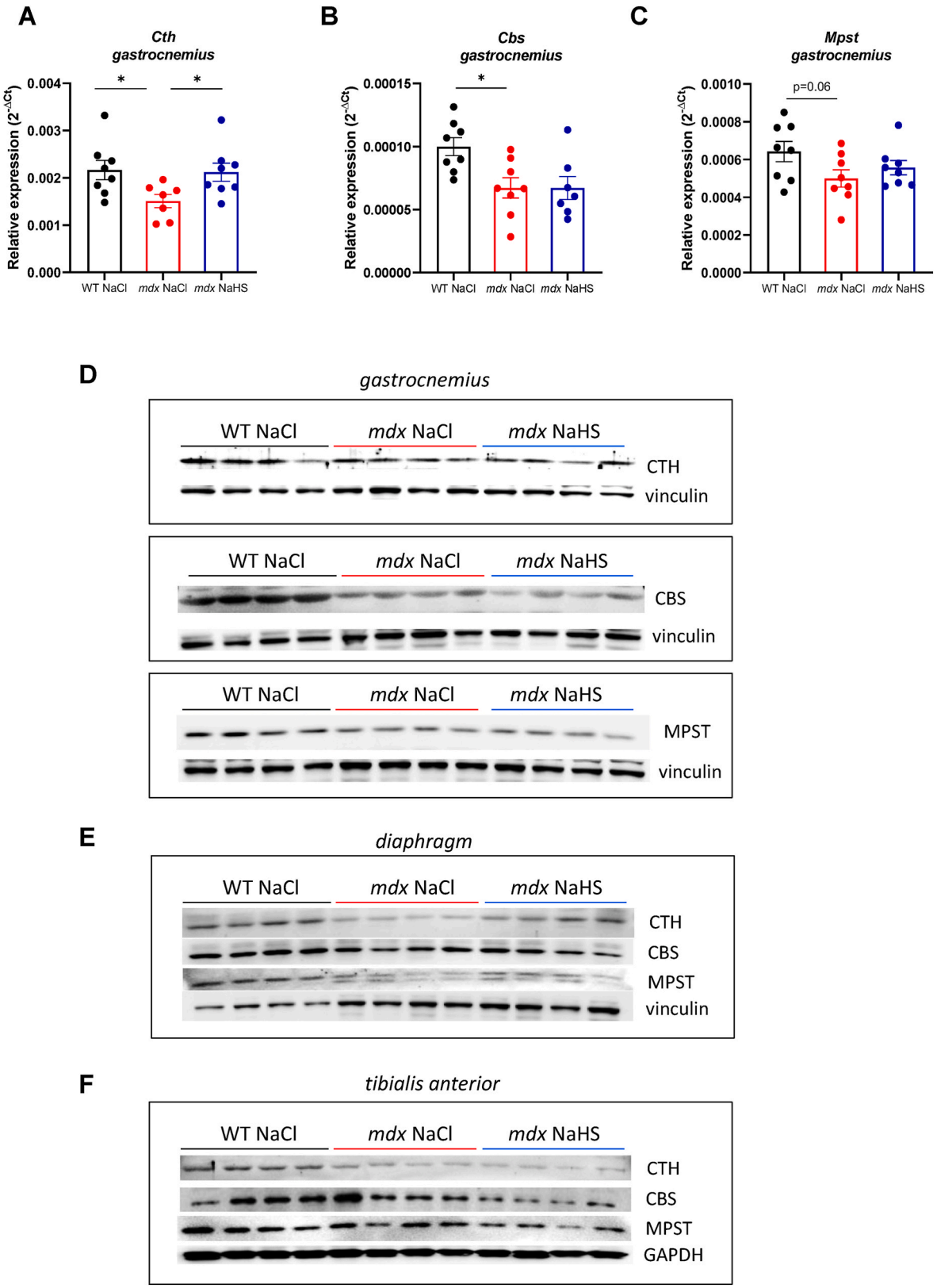

Fig. 1. The mRNA and protein level of H_2S-generating enzymes is decreased in *mdx* muscles, without prominent changes after NaHS treatment. The gene expression of *Cth* **(A)**, *Cbs* **(B)** and *Mpst* **(C)** is decreased in *mdx* gastrocnemius. The H_2S donor increased the expression of *Cth* transcript **(A)**. $n = 7–8$/group; qRT-PCR. The level of CTH, CBS and MPST was evaluated by Western blotting in the gastrocnemius **(D)**, diaphragm **(E)**, and tibialis anterior **(F)** muscles; vinculin or GAPDH were used as loading controls; $n = 4$/group. Results are shown as mean ± SEM; $^*p \leq 0.05$; one-way ANOVA with Tukey's post hoc test.

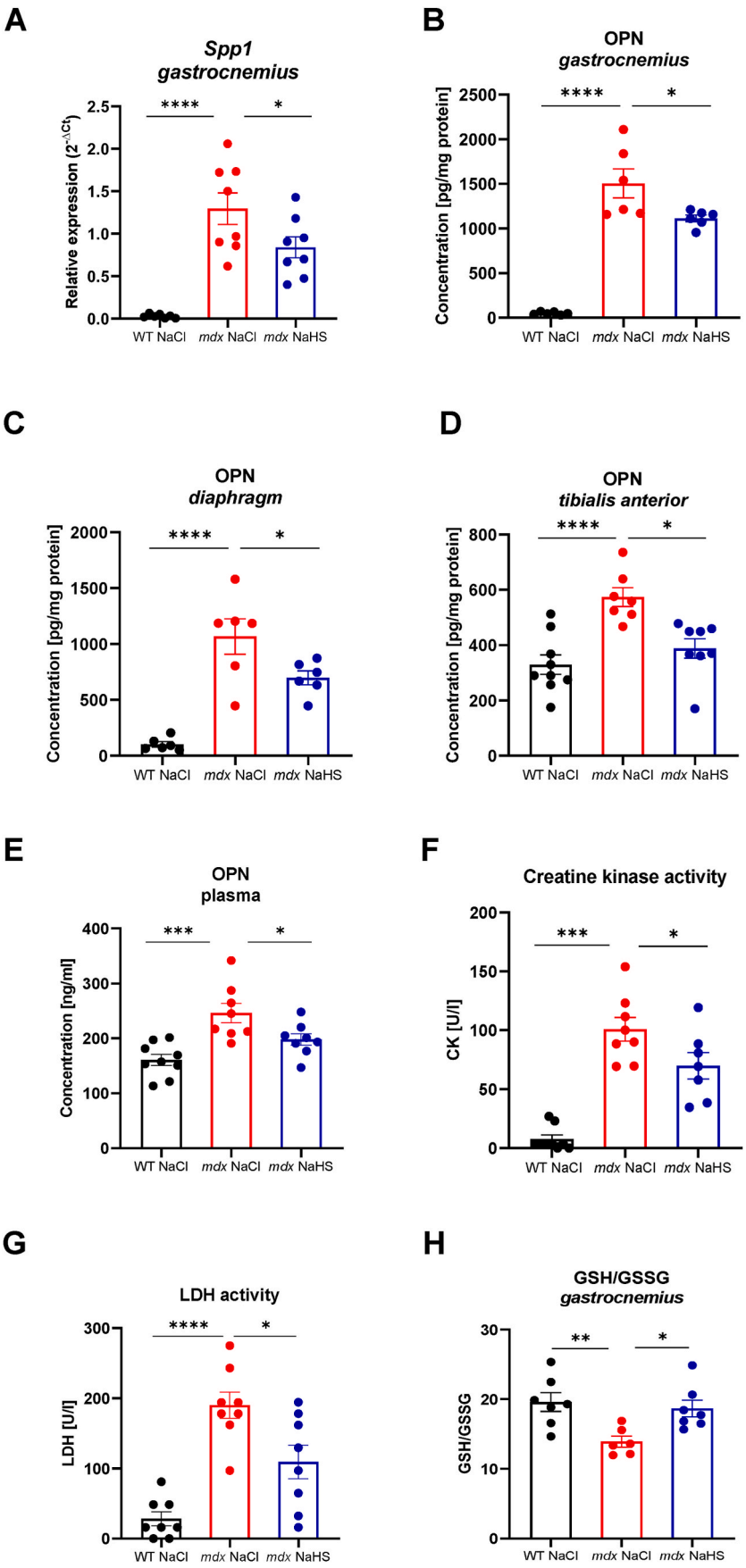

Fig. 2. Muscle damage markers in dystrophic mice are decreased by NaHS treatment, while the GSH/GSSH ratio is increased.

The upregulated expression of the *Spp1* gene (OPN transcript) in dystrophic gastrocnemius decreases after NaHS treatment **(A)**; qRT-PCR. Furthermore, NaHS reduced the elevated protein level of OPN in gastrocnemius **(B)**, diaphragm **(C)**, tibialis anterior **(D)** muscles and plasma **(E)**. The H_2S donor lowers the plasma activity of creatine kinase (CK) **(F)** and lactate dehydrogenase (LDH) **(G)** in *mdx* animals. NaHS treatment leads to increased GSH/GSSG ratio **(H)**. $n = 6–9$/group. Results are presented as mean ± SEM; $^{*}p \leq 0.05$; $^{**}p \leq 0.01$; $^{***}p \leq 0.001$; $^{****}p \leq 0.0001$; one-way ANOVA with Tukey's post hoc test.

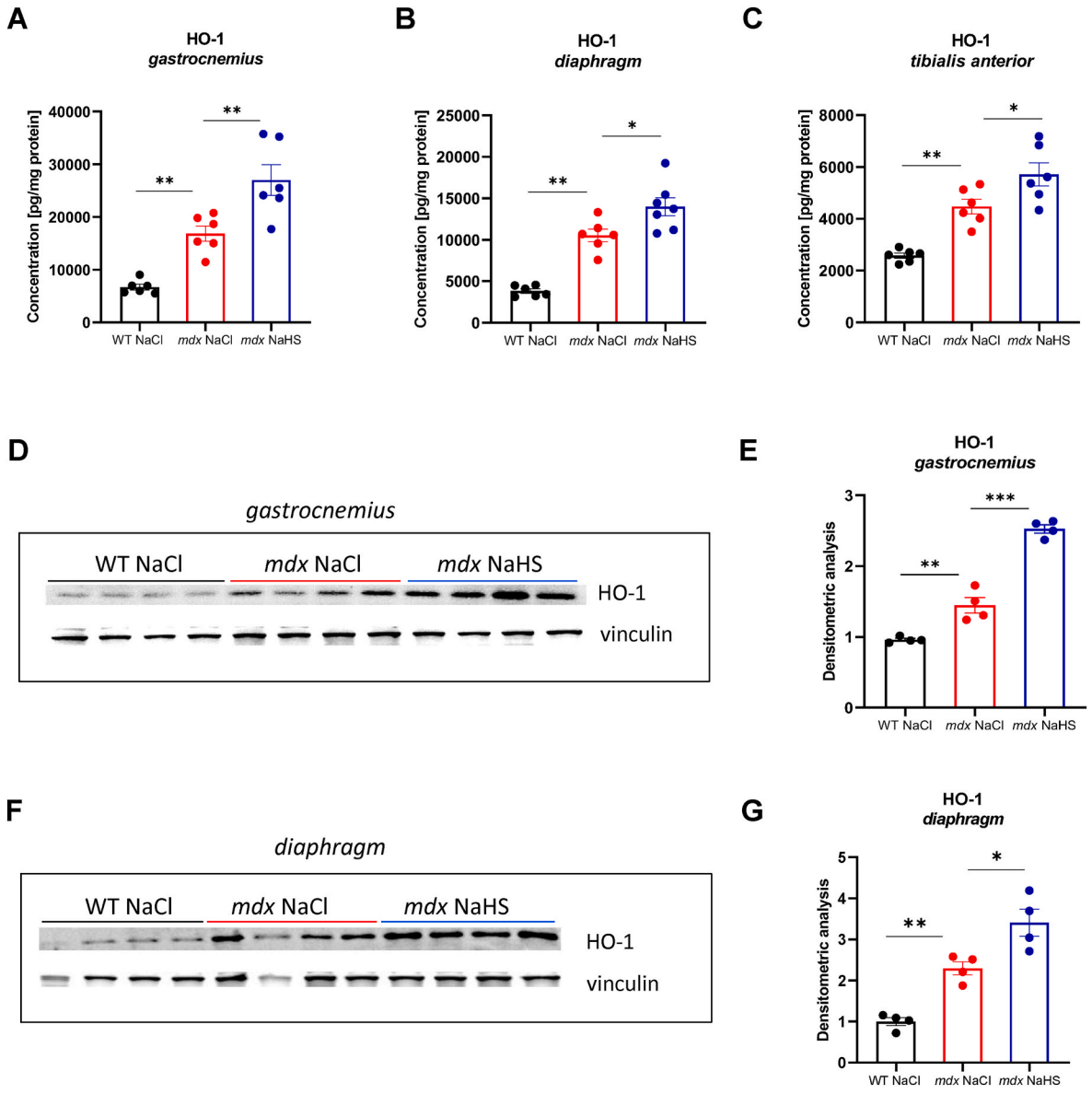

Fig. 3. NaHS up-regulates the antioxidant and anti-inflammatory heme oxygenase-1 level in dystrophic mice.
NaHS treatment up-regulates protein level of HO-1 as assessed by ELISA in the gastrocnemius **(A)**; diaphragm **(B)** and tibialis anterior **(C)** muscles; $n = 6–7$/group. Representative Western blots together with densitometric analyses of HO-1 protein level in gastrocnemius **(D, E)**, and diaphragm **(F, G)** muscles; vinculin was used as loading control; $n = 3–4$/group. Results are presented as mean ± SEM; $^{*}p \leq 0.05$; $^{**}p \leq 0.01$; $^{***}p \leq 0.001$; one-way ANOVA with Tukey's post hoc test.

sufficient to decrease the accumulation of inflammatory cells (Fig. 4E–K).

3.6. NaHS treatment down-regulates the expression of fibrotic factors in the tibialis anterior muscle, but collagen deposition in dystrophic mice remains unchanged

As we found a decrease in plasma and muscle levels of OPN (Fig. 2B–E), a factor that contributes to the regulation of fibrosis, to better understand the effect of NaHS treatment on this process, we analysed the expression of fibrotic factors both at the mRNA and protein level. As expected, the expression of transforming growth factor-1 β (*Tgfb1*, TGFβ), the main profibrotic factor, increased in dystrophic muscles (Fig. 5A, D, Supplementary Figs. 3A–D). Similarly, a potent increase in the expression of other factors, including the collagen type I alpha 1 chain (*Col1a1)* (Fig. 5B, E) and fibronectin 1 (*Fn1*) (Fig. 5C, F) was also noticed in dystrophic muscles. However, the effect of NaHS treatment was only found in the tibialis anterior (Fig. 5D–F). Interestingly, when TGFβ1 protein was evaluated in *mdx* mice (Supplementary Figs. 3B–D), again, the statistically significant decrease in its level after NaHS treatment was detected only in the tibialis anterior muscle.

To shed more light on this aspect, we performed Masson's trichrome staining and hydroxyproline measurement. We observed extensive collagen deposition in trichrome-stained dystrophic muscles, shown in the exemplary photos of gastrocnemius (Fig. 5G) and diaphragm (Supplementary Fig. 3E) and quantification in both muscles (Fig. 5H and I). No effect of NaHS supplementation was noticed (Fig. 5H and I, Supplementary Fig. 3F). Confirmatory results were obtained by the hydroxyproline assay, another indicator of collagen content, as no changes after NaHS, neither in the gastrocnemius (Supplementary Fig. 3G) nor in the tibialis anterior (Supplementary Fig. 3H) muscles were found.

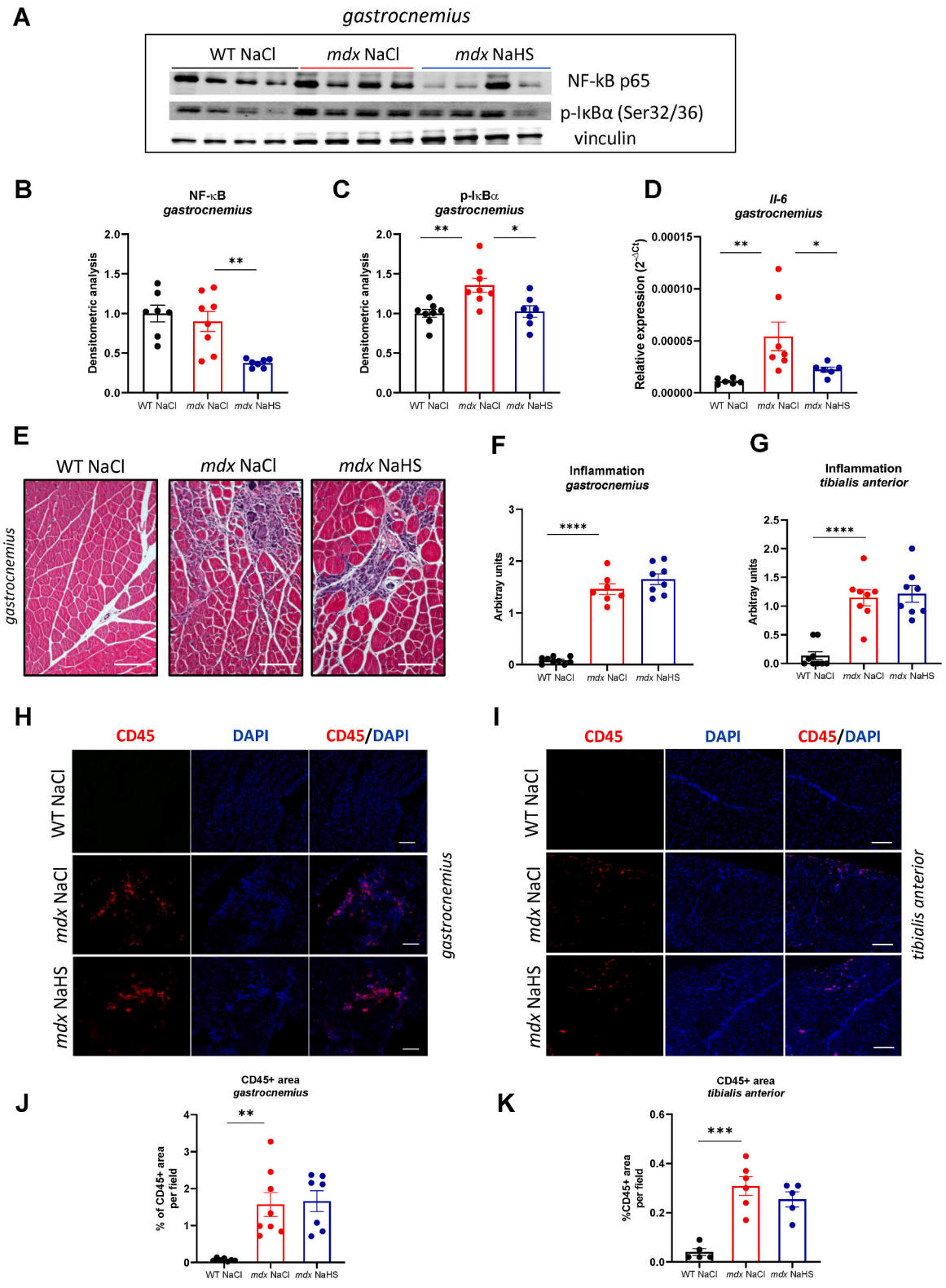

Fig. 4. The effect of NaHS on NF-κB signalling pathway and immune cell infiltration. Representative Western blot **(A)** with densitometric analysis showing lower level of NF-**κ**B protein **(B)** together with decreased phosphorylation of its inhibitor (IκB) **(C)** upon NaHS treatment. The expression of NF-κB-regulated *Il-6* is up-regulated in dystrophic muscle while decreases after the administration of NaHS **(D)**; $n = 6–8$/group. Representative pictures of H&E staining of the gastrocnemius **(E)** with semiquantitative analysis of the extent of inflammation in the gastrocnemius **(F)** and tibialis anterior **(G)** muscles, showing a potent increase in inflammatory cell infiltration in *mdx* mice without any effect of NaHS treatment; microscopic assessment using a Nikon Eclipse microscope. Scale bar: 100 μm; $n = 7–9$/group. Immunofluorescent detection of CD45, a pan-leukocyte marker: exemplary photos from the gastrocnemius muscle **(H)** and tibialis anterior **(I)** with semi-quantitative analysis in the gastrocnemius **(J)** and tibialis anterior **(K)** muscles; microscopic assessment using a Nikon Eclipse microscope. Scale bar: 100 μm; $n = 5–8$/group. Results are presented as mean ± SEM; $^{*}p \leq 0.05$; $^{**}p \leq 0.01$; $^{***}p \leq 0.001$; $^{****}p \leq 0.0001$; one-way ANOVA with Tukey's post hoc test.

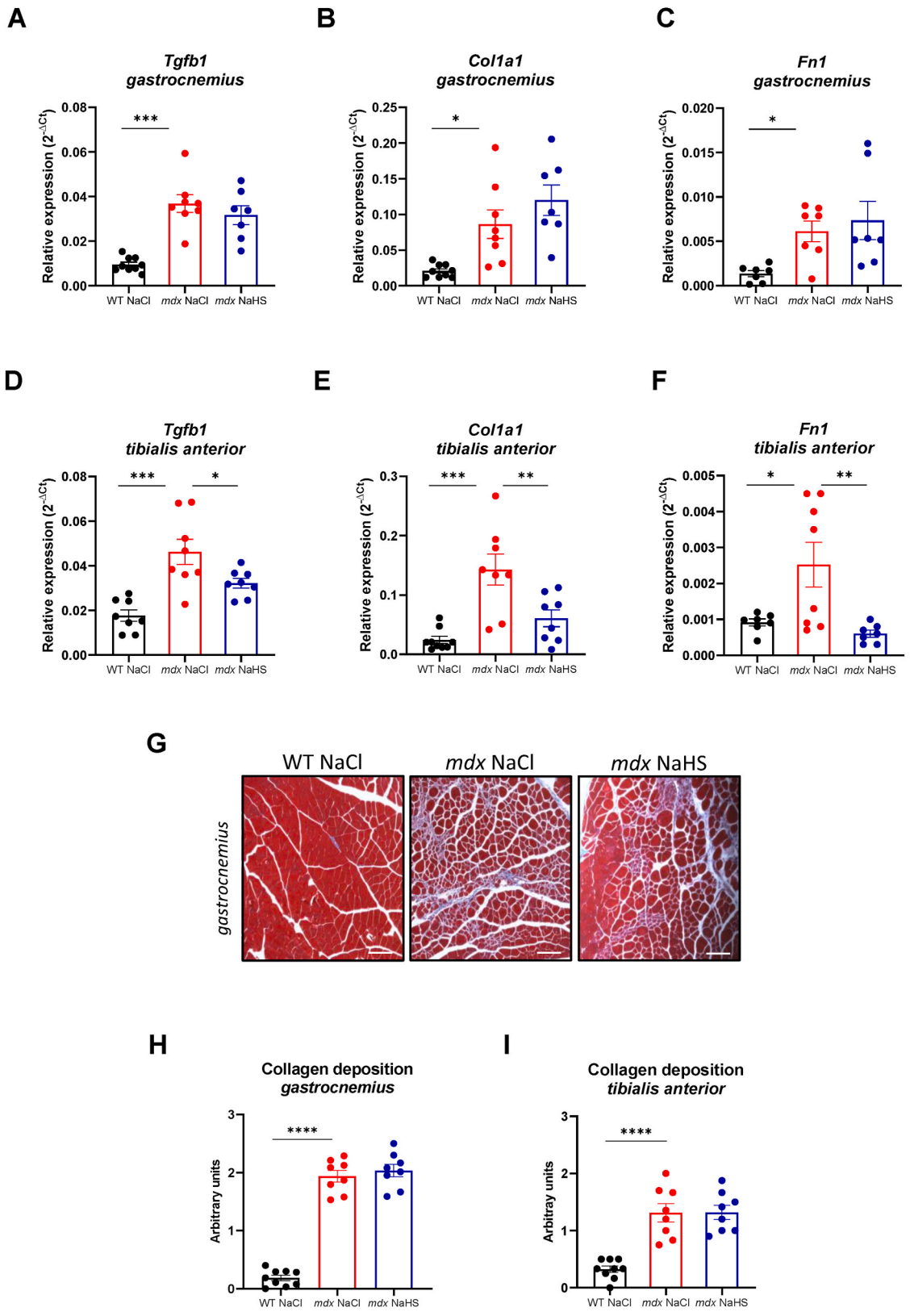

Fig. 5. Increased fibrosis in dystrophic muscles is not affected by NaHS treatment. Expression of fibrotic markers in WT, *mdx,* and NaHS-treated *mdx* animals: *Tgfb1* **(A, D)** *Col1a1* **(B, E)** and *Fn1* **(C, F)** in the gastrocnemius and the tibialis anterior muscles**,** respectively; $n = 7$–9/group; qRT-PCR. Representative photos of Masson's trichrome staining showing the accumulation of collagen in the gastrocnemius of *mdx* mice without the impact of NaHS treatment **(G)**; the semiquantitative analysis of collagen deposition in gastrocnemius **(H)**, diaphragm **(I)** and tibialis anterior **(J);** microscopic evaluation using a Nikon Eclipse microscope. Scale bar: 100 μm; $n =$ 8–9/group. Results are presented as mean ± SEM. *$p \leq 0.05$; **$p \leq 0.01$; ***$p \leq 0.001$; ****$p \leq 0.0001$; one-way ANOVA with Tukey's post hoc test.

3.7. NaHS treatment upregulates transcripts of angiogenic markers and the number of blood vessels in dystrophic gastrocnemius

As dysregulation of angiogenesis has been reported to be the important factor contributing to disease progression (Bronisz-Budzyńska et al., 2020, 2019, p. 14; Mucha et al., 2021b; Podkalicka et al., 2021, 2020) and H_2S can exert pro-angiogenic activities (Holwerda et al., 2014; Wang et al., 2010), our objective was to check the expression of some angiogenic factors in dystrophic muscles after NaHS delivery. The mRNA analysis revealed down-regulation of the main pro-angiogenic factor, vascular endothelial growth factor (*Vegfa*), and its receptor (*Kdr*) in dystrophic gastrocnemius (Fig. 6A, C) and tibialis anterior (Fig. 6B, D). NaHS treatment had a reversal effect on the expression of those factors only in the gastrocnemius muscle (Fig. 6A, C). However, when the protein level was analysed by ELISA, we did not find statistically significant differences in *mdx* mice treated with NaHS (Fig. 6E and F). Interestingly, we found an increase in the number of blood vessels positive for α-SMA/CD31/lectin after NaHS delivery in the gastrocnemius muscle (Fig. 6G and H).

3.8. Lack of the effect of NaHS on regeneration and muscle fiber composition in dystrophic mice

Disturbed angiogenesis in dystrophic muscles may contribute to

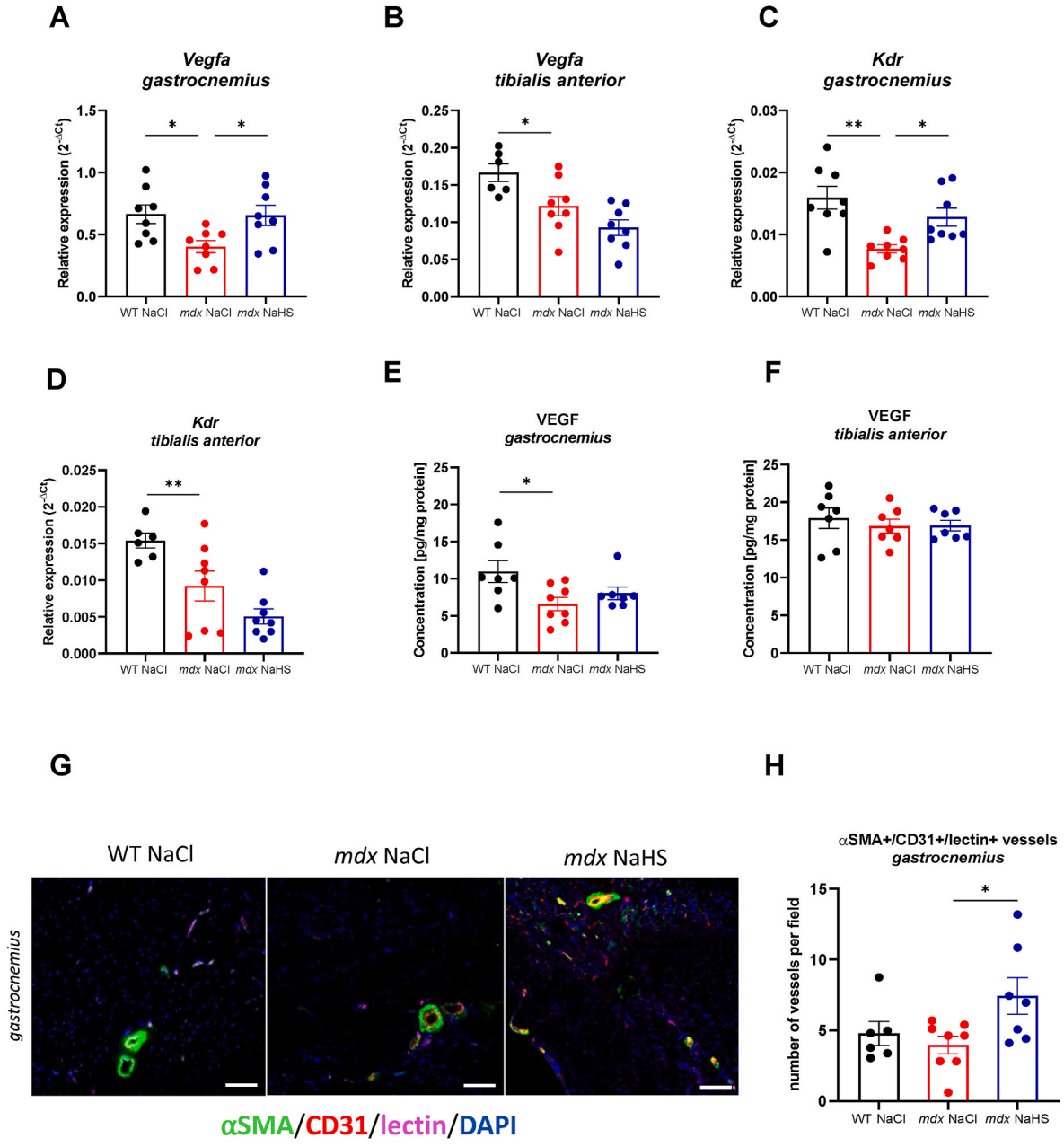

Fig. 6. NaHS affects the transcript levels of the angiogenic markers and the number of blood vessels in the dystrophic gastrocnemius muscle. Decreased mRNA level of angiogenesis-related genes *Vegfa* **(A, B)** and its receptor *Kdr* **(C, D)** in the gastrocnemius and tibialis anterior muscles of vehicle-treated *mdx* mice, respectively. The reversal effect after NaHS treatment on the expression of *Vegfa* **(A)** and *Kdr* **(C)** was evident only in the gastrocnemius; n = 6–8/group; qRT-PCR. Protein level measurement of VEGF (ELISA) showed its decreased level in gastrocnemius of *mdx* mice **(E)** with no effect in tibialis anterior muscle **(F)**; n = 7/group. Immunofluorescent analysis of gastrocnemius confirmed increased number of blood vessels positive for CD31 (to visualise endothelial cells); α-SMA (for smooth muscle cells identification) and lectin (binds to glycoproteins in glycocalyx and in the basal membrane of endothelial cells) after NaHS treatment **(G, H)**; n = 6–8/group. Scale bar: 100 μm. Results are presented as mean ± SEM; *$p \leq 0.05$; **$p \leq 0.01$; one-way ANOVA with Tukey's post hoc test.

impaired regeneration. To analyse muscle fiber regeneration capacity, we evaluated the presence of centrally nucleated fibers (CNF). Similarly to our previous studies (Mucha et al., 2021b; Podkalicka et al., 2020), in the present work, we found a higher percentage of CNF in all analysed dystrophic muscles, but no changes were noticed after NaHS treatment (Fig. 7A–D). In addition, the protein level of FGF2, reported to be upregulated during regeneration (Anderson et al., 1995), was significantly changed by NaHS neither in the *mdx* gastrocnemius (Supplementary Fig. 3I) nor in the tibialis anterior (Supplementary Fig. 3J). Furthermore, NaHS treatment did not affect the expression of the embryonic myosin heavy chain isoform *Myh3*, which encodes eMyHC, a marker of regenerating myofibers, potently increased in the dystrophin-lacking muscles (Fig. 7E–G).

Finally, to check whether NaHS affects muscle fiber composition, we performed NADH dehydrogenase activity assessment to distinguish oxidative (dark) and nonoxidative (pale) fibers. As in our previous analysis (Podkalicka et al., 2020), the number of $NADH^+$ fibers was noticeably increased in *mdx* animals; however no effect of NaHS was detected in gastrocnemius muscle (Fig. 7H and I).

3.9. Administration of NaHS regulates autophagy markers in dystrophic gastrocnemius but does not affect muscle strength

Impaired autophagy has been demonstrated to be another hallmark of DMD (Mucha et al., 2021a; Pal et al., 2014), and a recent study suggests that NaHS may regulate autophagy markers in *mdx* mice (Panza et al., 2021). In our hands, increased activation of α subunit of AMP-activated protein kinase (AMPKα) known to regulate autophagy was evident in *mdx* gastrocnemius muscle with further up-regulation after NaHS treatment (Fig. 8A and B). Moreover, NaHS tended to increase or increased the expression of autophagy-related genes (*Atg)* such as *Atg5* and *Atg7,* respectively (Fig. 8C and D). In contrast, the p-AMPKα/AMPKα ratio was not regulated by NaHS in dystrophic diaphragm (Fig. 8 E, F).

Finally, taking into consideration the versatile effects of AMPK signaling and the possible effect of NaHS on different pathways, we evaluated if H_2S donor is able to affect the impaired muscle functions. However, no apparent improvement in the reduced grip strength of dystrophin-deficient mice was found after NaHS administration (Fig. 8G).

4. Discussion

DMD remains an incurable and fatal disease that leads to premature death. Current strategies for DMD treatment are based on pharmacological, gene, and cell approaches. Unfortunately, all of them have serious limitations (Łoboda and Dulak, 2020). Therefore, it is necessary to look for novel pharmacological compounds, especially those that can provide broad therapeutic benefits and counteract the hallmark symptoms of DMD related to excessive inflammation, oxidative stress, fibrosis, altered autophagy, and angiogenesis. The pleiotropic agent, H_2S, can be considered a candidate compound. Many studies have demonstrated its anti-inflammatory (Bhatia and Gaddam, 2021), anti-apoptotic (Wetzel and Wenke, 2019), and antioxidant properties (Shefa et al., 2018), with a well-established role in angiogenesis (Wu et al., 2018) or smooth muscle contractility (Tang et al., 2006). We noticed that dystrophin deficiency leads to decreased expression of H_2S generating enzymes in different muscle types, which can be postulated as a new hallmark of DMD. Similarly, Panza et al. (2021) showed defective transsulfuration pathway activity in *mdx* animals and also in human myoblasts isolated from DMD donors. Ellwood et al. (2021) also demonstrated reduced levels of H_2S-producing enzymes in a more severe mouse model with dystrophin and utrophin deficiency. Additionally, Bitar et al. (2018) identified diabetes-induced diminished expression of H_2S generating enzymes and a decreased level of the CTH protein in sarcopenic muscles, pointing toward the role of H_2S in different models of muscle pathology. It should be noted that the exact mechanism underlying how dystrophin deficiency leads to reduced expression of these enzymes needs further investigation; however, based on these results we postulated that an H_2S donor may ameliorate muscle pathology in a mouse model of DMD.

The salient finding of the present study is that treatment with a fast-releasing H_2S donor, NaHS, regulates the expression of genes and proteins associated with DMD. Interestingly, the possible role of this gaseous mediator in DMD has not been examined until recently. Panza et al. (2021) found that NaHS has a positive effect on muscle functions in 7-week-old and 17-week-old *mdx* mice, through modulation of inflammatory and fibrotic markers, as well as autophagy regulators. Saclier et al. (2021) reported that treatment of *mdx* mice with the same donor for 3 weeks resulted in a very moderate difference in collagen accumulation; however, it dampened inflammation. In *C. elegans* with a nonsense mutation at position 3287 of the DYS-1 dystrophin ortholog, Ellwood et al. (2021) used two types of H_2S donors, a slow-release sodium GYY4137 (NaGYY) and AP39, which targets H_2S delivery to mitochondria. This supplementation was able to improve functional defects in movement, strength, and gait of dystrophic worms (Ellwood et al., 2021).

Our work confirms some of the previously published effects, but we also revealed new possible mechanisms of NaHS action in DMD. Importantly, we found decreased level of DMD plasma markers, like CK, LDH and OPN, with the latter regulated by NaHS also in muscles. We demonstrated the improved antioxidant properties of *mdx* animals after NaHS treatment, which involved an increase in the GSH/GSSG ratio and HO-1 expression accompanied by down-regulation of the NF-κB signalling pathway. These mechanisms were not fully evaluated in previous studies on the role of H_2S in DMD (Ellwood et al., 2021; Panza et al., 2021; Saclier et al., 2021).

Angiogenesis has been implicated in the progression of DMD. We (Podkalicka et al., 2021) and others (Latroche et al., 2015) have previously shown age-dependent abnormalities in the structure and functions of blood vessels in dystrophic mice. In the present work, we have also demonstrated diminished expression of VEGF in *mdx* animals. Importantly, we found that NaHS administration increased *Vegfa* and its receptor *Kdr* (*Vegfr2*) gene expression in dystrophic gastrocnemius, indicating this regulation of special interest in future work. Not only was the expression of angiogenic factors modified in this muscle, but also the number of blood vessels was higher after NaHS. Although H_2S has been described as a molecule that promotes angiogenesis (Cheng and Kishore, 2020), this aspect has not previously been investigated in dystrophic animals. Our study suggests for the first time that modulation of angiogenesis could be a new mechanism for the beneficial effect of NaHS in the treatment of DMD.

In addition to insufficient angiogenesis, our group recently demonstrated age-dependent alterations in the expression of autophagy-related genes and proteins under dystrophic conditions (Mucha et al., 2021a). Both insufficient and excessive autophagy can contribute to muscle atrophy (Sandri, 2010). Moreover, an improvement in autophagy was proposed as a strategy to attenuate DMD (De Palma et al., 2014). In the present work, we demonstrate that NaHS promotes the activation of AMPKα, as assessed by the increased ratio of phosphorylated AMPKα to total AMPKα. Recently, the regulatory role of H_2S donors in the autophagy process was proved (reviewed in (Wang et al., 2019):), and H_2S was found to activate AMPK through Cys302-dependent S-sulfuration (Hou et al., 2021). Furthermore, we showed that NaHS administration increased the expression of *Atg5* and *Atg7* genes. Restoration of autophagy in dystrophic skeletal muscle tissues after NaHS delivery was also indicated earlier (Panza et al., 2021). As AMPK regulates lipid and glucose metabolism and serves as a metabolic sensor, the effect of H_2S donors on this pathway may have a much wider outcome, not only related to autophagy regulation.

In sum, we demonstrated some protective effects of NaHS treatment; however, selected aspects of DMD pathology were moderately or not

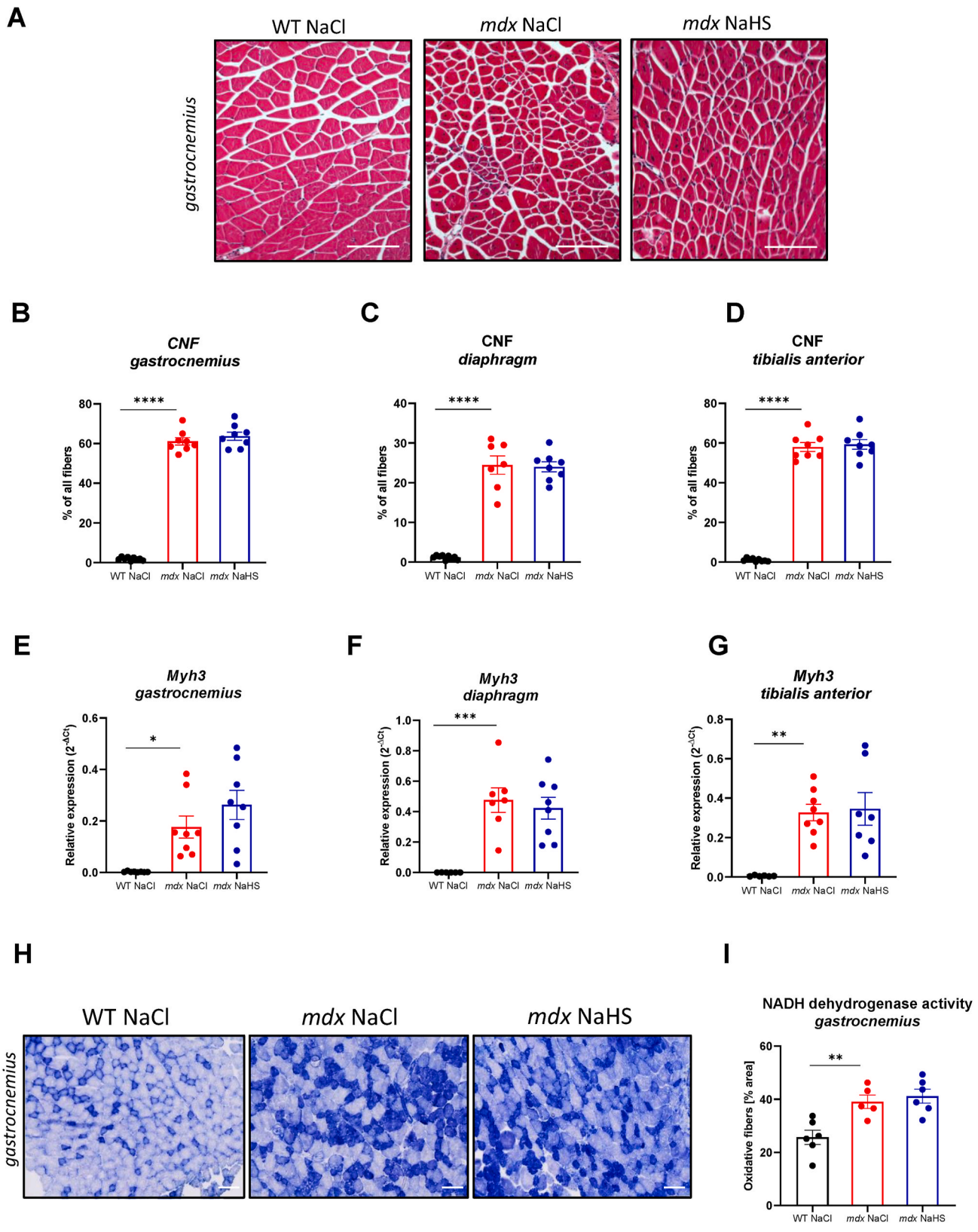

Fig. 7. NaHS neither regulates muscle regeneration nor affects muscle fiber composition. Representative photos **(A)** and semiquantitative analysis of centrally nucleated fibers (CNF) performed based on H&E staining showing a prominent increase in their number in gastrocnemius **(B)**, diaphragm **(C)** and tibialis anterior **(D)** muscles of *mdx* animals, which is not affected by NaHS treatment; scale bar: 100 μm; $n = 7–9$/group. Expression of myosin heavy chain isoform-coding gene (*Myh3)* in various muscles **(E–G)**; $n = 6–8$; qRT-PCR. Representative pictures of histochemical staining **(H)** and semiquantitative analysis **(I)** of NADH dehydrogenase activity to evaluate the extent of oxidative (dark) and non-oxidative (pale) fibers and the effect of NaHS. Although the number of NADH + fibers was markedly increased in *mdx* animals, no influence of NaHS was evident in the gastrocnemius muscle; scale bar: 100 μm; $n = 5–6$/group. Results are presented as mean ± SEM; $^{**}p \leq 0.01$; $^{***}p \leq 0.001$; $^{****}p \leq 0.0001$; one-way ANOVA with Tukey's post hoc test.

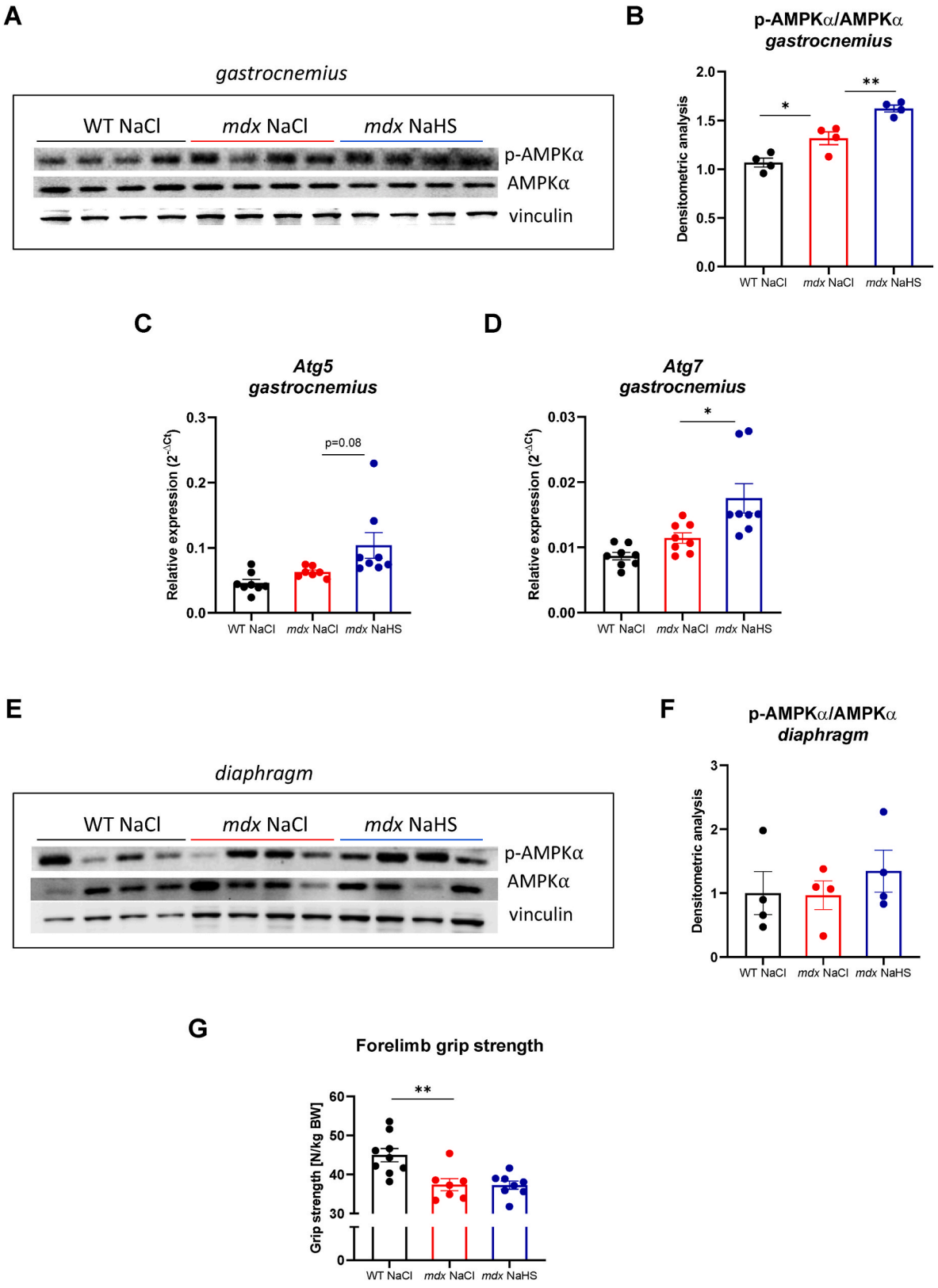

Fig. 8. The effect of NaHS on autophagy markers. Representative Western blot **(A)** with densitometric analysis **(B)** showing an up-regulation of the ratio of p-AMPKα/AMPKα after NaHS treatment in *mdx* animals; $n = 4$/group. As assessed by qRT-PCR, NaHS tended to increase the expression of *Atg5* **(C)** and up-regulated the level of *Atg7* **(D)**; $n = 8$–9/group. The p-AMPKα/AMPKα ratio was also assessed in the diaphragm **(E, F)** but the effect of NaHS was not evident. The decrease in forelimb grip strength in *mdx* mice, shown as the values normalized to body weight (N/kg BW), is not reversed after NaHS treatment **(G)**; $n = 5$–9/group. Results are presented as mean ± SEM; $^{*}p \leq 0.05$; $^{**}p \leq 0.01$; one-way ANOVA with Tukey's post hoc test.

influenced. Some of the results did not confirm previously published data, and one can speculate that this may result from slight discrepancies in the applied methodology, including the age and genetic background of the mice, as well as the dose and duration of NaHS treatment. However, a detailed analysis of these parameters did not reveal dramatic differences in the experimental settings. Although Saclier et al. (2021) utilized another mouse model called *DMD*^{mdx4Cv}, the genetic background was the same as used in our and Panza et al. (2021) studies (WT - C57BL/10ScSnJ and *mdx* - C57BL/10ScSn-DMD*mdx*/J). The effectiveness of treatment may also be related to the duration and dose of H_2S donor delivery. While Saclier et al. (2021) injected NaHS (1 mg/kg) or PBS daily intraperitoneally in 10- to 12-week-old *mdx* mice for 3 weeks, Panza et al. (2021) used three times higher doses of NaHS (3 mg/kg) once a day in two schemes: for 2 weeks (from 5 to 7 weeks) and 12 weeks (from 5 to 17 weeks of age) by oral gavage. In our hands, intraperitoneal administration of 100 μmol/kg/day (5.6 mg/kg/day) NaHS was started in 5-6-week-old animals and lasted 5 weeks. It has to be stressed, that although the dose of 100 μmol/kg/day is considered therapeutic in various disease models (Gomez et al., 2019; Ng et al., 2017; Yu et al., 2015), in dystrophic animals, the dose necessary to exert better protective effects might differ Therefore, future work should test other protocols, including the dose, scheme, regimen, and age of the animals.

5. Conclusions

In our hands, NaHS treatment attenuated hallmarks of DMD such as increased oxidative stress, fibrosis and inflammatory signalling, altered angiogenesis, and autophagy in a mouse *mdx* model. However, it did not fully restore the pathology of DMD and some effects were muscle-dependent. Due to the powerful potential of H_2S as a cytoprotective molecule, its impact on dystrophic muscles warrants further investigation.

6. Study limitations and future perspectives

First, as mentioned above, in our study we used a literature-based concentration of NaHS. Testing various experimental schemes, including different doses of NaHS in *mdx* animals, would provide additional information on the effect of this donor on the pathology of DMD. Consequently, the pharmacology of NaHS in dystrophic muscle would be an important aspect of such a study. Second, although we have shown beneficial effects of treatment, a further evaluation of muscle strength would also extend our understanding of the role of H_2S in the progression of DMD. In particular, the cardioprotective effects of the donor should also be addressed, as the main cause of premature death of DMD patients is related to cardiorespiratory dysfunction and the development of cardiomyopathy. Ideally, in patients with DMD, the condition of both skeletal muscle and the heart muscle should be improved by the possible drug. Third, this analysis only includes one selected donor, which has several limitations; for example, it hydrolyses immediately upon dissolution in water and releases H_2S in a rapid way. Therefore, the use of NaHS can have limited therapeutic potential. The current availability of slow-releasing donors that specifically target selected tissues may be the better option.

Funding

This work was supported by grant #2019/35/B/NZ3/02817 (to AŁ) from the National Science Centre.

Ethics statement

The animal experiments were approved by the 2nd Institutional Animal Care and Use Committee (IACUC) in Kraków, Poland (approval number 261/2020).

CRediT authorship contribution statement

Małgorzata Myszka: Investigation, Writing – original draft. **Olga Mucha:** Investigation. **Paulina Podkalicka:** Investigation. **Urszula Waśniowska:** Investigation. **Józef Dulak:** Formal analysis, Writing – review & editing. **Agnieszka Łoboda:** Formal analysis, Conceptualization, Data curation, Funding acquisition, Investigation, Project administration, Supervision, Writing – original draft, Writing – review & editing.

Declaration of competing interest

The authors declare that there are no competing interests associated with the manuscript.

Data availability

No data was used for the research described in the article.

Acknowledgments

We would like to acknowledge Ewa Werner, Karolina Hajduk, Karolina Kordeczka, Łukasz Szczepanik and Janusz Drebot from the Animal Facility for mice care and breeding. We would like to thank the administrative staff (Agnieszka Andrychowicz-Róg, Joanna Uchto-Bajołek and Joanna Strzęp-Knapiak) for their assistance. The technical help of students (Maria Bryczek, Ewa Jakubczak Kalina Hajok, Katarzyna Kaziród, Gabriela Owca) is highly acknowledged.

Abbreviations

AMPK – AMP activated protein kinase
CK – Creatine kinase
Col1a1 – Collagen type I alpha 1
CNF – Centrally nucleated fibers
CTH – Cystathionine γ-lyase
DMD – Duchenne muscular dystrophy
FGF2 – Fibroblast growth factor-2
HO-1 – Heme oxygenase-1
H_2S – Hydrogen sulfide;
Kdr – VEGF receptor 2 (VEGF-R2)
LDH – Lactate dehydrogenase
NaHS – Sodium hydrosulfide;
NF-κB – Nuclear factor kappa-light-chain-enhancer of activated B cells
***Spp1*, OPN** – Secreted phosphoprotein 1, osteopontin
TGF-β1 – Transforming growth factor-beta 1
***Vegfa*, VEGF** – Vascular endothelial growth factor

Appendix A. Supplementary data

Supplementary data to this article can be found online at https://doi.org/10.1016/j.ejphar.2023.175928.

References

Aartsma-Rus, A., van Putten, M., 2014. Assessing functional performance in the mdx mouse model. J Vis Exp 85, 51303. https://doi.org/10.3791/51303.

Anderson, J.E., Mitchell, C.M., McGeachie, J.K., Grounds, M.D., 1995. The time course of basic fibroblast growth factor expression in crush-injured skeletal muscles of SJL/J and BALB/c mice. Exp. Cell Res. 216, 325–334. https://doi.org/10.1006/excr.1995.1041.

Bhatia, M., Gaddam, R.R., 2021. Hydrogen sulfide in inflammation: a novel mediator and therapeutic target. Antioxid. Redox Signal. 34, 1368–1377. https://doi.org/10.1089/ars.2020.8211.

Birnkrant, D.J., Bushby, K., Bann, C.M., Apkon, S.D., Blackwell, A., Brumbaugh, D., Case, L.E., Clemens, P.R., Hadjiyannakis, S., Pandya, S., Street, N., Tomezsko, J., Wagner, K.R., Ward, L.M., Weber, D.R., DMD Care Considerations Working Group, 2018. Diagnosis and management of Duchenne muscular dystrophy, part 1: diagnosis, and neuromuscular, rehabilitation, endocrine, and gastrointestinal and

nutritional management. Lancet Neurol. 17, 251–267. https://doi.org/10.1016/S1474-4422(18)30024-3.
Bitar, M.S., Nader, J., Al-Ali, W., Al Madhoun, A., Arefanian, H., Al-Mulla, F., 2018. Hydrogen sulfide donor NaHS improves metabolism and reduces muscle atrophy in type 2 diabetes: implication for understanding sarcopenic pathophysiology. Oxid. Med. Cell. Longev. 2018, 6825452 https://doi.org/10.1155/2018/6825452.
Bladen, C.L., Salgado, D., Monges, S., Foncuberta, M.E., Kekou, K., Kosma, K., Dawkins, H., Lamont, L., Roy, A.J., Chamova, T., Guergueltcheva, V., Chan, S., Korngut, L., Campbell, C., Dai, Y., Wang, J., Barišić, N., Brabec, P., Lahdetie, J., Walter, M.C., Schreiber-Katz, O., Karcagi, V., Garami, M., Viswanathan, V., Bayat, F., Buccella, F., Kimura, E., Koeks, Z., van den Bergen, J.C., Rodrigues, M., Roxburgh, R., Lusakowska, A., Kostera-Pruszczyk, A., Zimowski, J., Santos, R., Neagu, E., Artemieva, S., Rasic, V.M., Vojinovic, D., Posada, M., Bloetzer, C., Jeannet, P.-Y., Joncourt, F., Díaz-Manera, J., Gallardo, E., Karaduman, A.A., Topaloğlu, H., El Sherif, R., Stringer, A., Shatillo, A.V., Martin, A.S., Peay, H.L., Bellgard, M.I., Kirschner, J., Flanigan, K.M., Straub, V., Bushby, K., Verschuuren, J., Aartsma-Rus, A., Béroud, C., Lochmüller, H., 2015. The TREAT-NMD DMD Global Database: analysis of more than 7,000 Duchenne muscular dystrophy mutations. Hum. Mutat. 36, 395–402. https://doi.org/10.1002/humu.22758.
Bronisz-Budzyńska, I., Chwalenia, K., Mucha, O., Podkalicka, P., Bukowska-Strakova, K., Józkowicz, A., Łoboda, A., Kozakowska, M., Dulak, J., 2019. miR-146a deficiency does not aggravate muscular dystrophy in mdx mice. Skeletal Muscle 9, 22. https://doi.org/10.1186/s13395-019-0207-0.
Bronisz-Budzyńska, I., Kozakowska, M., Podkalicka, P., Kachamakova-Trojanowska, N., Łoboda, A., Dulak, J., 2020. The role of Nrf2 in acute and chronic muscle injury. Skeletal Muscle 10, 35. https://doi.org/10.1186/s13395-020-00255-0.
Bulfield, G., Siller, W.G., Wight, P.A., Moore, K.J., 1984. X chromosome-linked muscular dystrophy (mdx) in the mouse. Proc. Natl. Acad. Sci. U. S. A. 81, 1189–1192. https://doi.org/10.1073/pnas.81.4.1189.
Carter, J.C., Sheehan, D.W., Prochoroff, A., Birnkrant, D.J., 2018. Muscular dystrophies. Clin. Chest Med. 39, 377–389. https://doi.org/10.1016/j.ccm.2018.01.004.
Cheng, Z., Kishore, R., 2020. Potential role of hydrogen sulfide in diabetes-impaired angiogenesis and ischemic tissue repair. Redox Biol. 37, 101704 https://doi.org/10.1016/j.redox.2020.101704.
Chomczynski, P., Sacchi, N., 1987. Single-step method of RNA isolation by acid guanidinium thiocyanate-phenol-chloroform extraction. Anal. Biochem. 162, 156–159. https://doi.org/10.1006/abio.1987.9999.
De Palma, C., Morisi, F., Cheli, S., Pambianco, S., Cappello, V., Vezzoli, M., Rovere-Querini, P., Moggio, M., Ripolone, M., Francolini, M., Sandri, M., Clementi, E., 2014. Autophagy as a new therapeutic target in Duchenne muscular dystrophy. Cell Death Dis. 5, e1363. https://doi.org/10.1038/cddis.2014.312.
Dulak, J., 2021. Gene therapy. The legacy of Wacław Szybalski. Acta Biochim. Pol. 68, 359–375. https://doi.org/10.18388/abp.2020_5805.
Ellwood, R.A., Hewitt, J.E., Torregrossa, R., Philp, A.M., Hardee, J.P., Hughes, S., van de Klashorst, D., Gharahdaghi, N., Anupom, T., Slade, L., Deane, C.S., Cooke, M., Etheridge, T., Piasecki, M., Antebi, A., Lynch, G.S., Philp, A., Vanapalli, S.A., Whiteman, M., Szewczyk, N.J., 2021. Mitochondrial hydrogen sulfide supplementation improves health in the *C. elegans* Duchenne muscular dystrophy model. Proc. Natl. Acad. Sci. U.S.A. 118, e2018342118 https://doi.org/10.1073/pnas.2018342118.
Emery, A.E.H., 2002. The muscular dystrophies. Lancet 359, 687–695. https://doi.org/10.1016/S0140-6736(02)07815-7.
Gao, Q.Q., McNally, E.M., 2015. The dystrophin complex: structure, function, and implications for therapy. In: Terjung, R. (Ed.), Comprehensive Physiology. Wiley, pp. 1223–1239. https://doi.org/10.1002/cphy.c140048.
Giuffrè, A., Vicente, J.B., 2018. Hydrogen sulfide biochemistry and interplay with other gaseous mediators in mammalian physiology. Oxid. Med. Cell. Longev., 6290931 https://doi.org/10.1155/2018/6290931, 2018.
Gomez, C.B., de la Cruz, S.H., Medina-Terol, G.J., Beltran-Ornelas, J.H., Sánchez-López, A., Silva-Velasco, D.L., Centurión, D., 2019. Chronic administration of NaHS and L-Cysteine restores cardiovascular changes induced by high-fat diet in rats. Eur. J. Pharmacol. 863, 172707 https://doi.org/10.1016/j.ejphar.2019.172707.
Hoffman, E.P., Brown, R.H., Kunkel, L.M., 1987. Dystrophin: the protein product of the Duchenne muscular dystrophy locus. Cell 51, 919–928. https://doi.org/10.1016/0092-8674(87)90579-4.
Holwerda, K.M., Burke, S.D., Faas, M.M., Zsengeller, Z., Stillman, I.E., Kang, P.M., van Goor, H., McCurley, A., Jaffe, I.Z., Karumanchi, S.A., Lely, A.T., 2014. Hydrogen sulfide attenuates sFlt1-induced hypertension and renal damage by upregulating vascular endothelial growth factor. J. Am. Soc. Nephrol. 25, 717–725. https://doi.org/10.1681/ASN.2013030291.
Hou, X.-O., Tu, H.-Y., Qian, H.-C., Li, Q., Yang, Y.-P., Xu, G.-Q., Wang, F., Liu, C.-F., Wang, Y.-L., Hu, L.-F., 2021. AMPK S-sulfuration contributes to H2S donors-induced AMPK phosphorylation and autophagy activation in dopaminergic cells. Neurochem. Int. 150, 105187 https://doi.org/10.1016/j.neuint.2021.105187.
Kornegay, J.N., Childers, M.K., Bogan, D.J., Bogan, J.R., Nghiem, P., Wang, J., Fan, Z., Howard, J.F., Schatzberg, S.J., Dow, J.L., Grange, R.W., Styner, M.A., Hoffman, E.P., Wagner, K.R., 2012. The paradox of muscle hypertrophy in muscular dystrophy. Phys. Med. Rehabil. Clin 23, 149–172. https://doi.org/10.1016/j.pmr.2011.11.014 xii.
Kozakowska, M., Pietraszek-Gremplewicz, K., Ciesla, M., Seczynska, M., Bronisz-Budzynska, I., Podkalicka, P., Bukowska-Strakova, K., Loboda, A., Jozkowicz, A., Dulak, J., 2018. Lack of heme oxygenase-1 induces inflammatory reaction and proliferation of muscle satellite cells after cardiotoxin-induced skeletal muscle injury. Am. J. Pathol. 188, 491–506. https://doi.org/10.1016/j.ajpath.2017.10.017.
Kuraoka, M., Kimura, E., Nagata, T., Okada, T., Aoki, Y., Tachimori, H., Yonemoto, N., Imamura, M., Takeda, S., 2016. Serum osteopontin as a novel biomarker for muscle regeneration in Duchenne muscular dystrophy. Am. J. Pathol. 186, 1302–1312. https://doi.org/10.1016/j.ajpath.2016.01.002.
Latroche, C., Matot, B., Martins-Bach, A., Briand, D., Chazaud, B., Wary, C., Carlier, P.G., Chrétien, F., Jouvion, G., 2015. Structural and functional alterations of skeletal muscle microvasculature in dystrophin-deficient mdx mice. Am. J. Pathol. 185, 2482–2494. https://doi.org/10.1016/j.ajpath.2015.05.009.
Łoboda, A., Dulak, J., 2020. Muscle and cardiac therapeutic strategies for Duchenne muscular dystrophy: past, present, and future. Pharmacol. Rep. 72, 1227–1263. https://doi.org/10.1007/s43440-020-00134-x.
Mucha, O., Kaziród, K., Podkalicka, P., Rusin, K., Dulak, J., Łoboda, A., 2021a. Dysregulated autophagy and mitophagy in a mouse model of Duchenne muscular dystrophy remain unchanged following heme oxygenase-1 knockout. Int. J. Mol. Sci. 23, 470. https://doi.org/10.3390/ijms23010470.
Mucha, O., Podkalicka, P., Kaziród, K., Samborowska, E., Dulak, J., Łoboda, A., 2021b. Simvastatin does not alleviate muscle pathology in a mouse model of Duchenne muscular dystrophy. Skeletal Muscle 11, 21. https://doi.org/10.1186/s13395-021-00276-3.
Ng, H.H., Yildiz, G.S., Ku, J.M., Miller, A.A., Woodman, O.L., Hart, J.L., 2017. Chronic NaHS treatment decreases oxidative stress and improves endothelial function in diabetic mice. Diabetes Vasc. Dis. Res. 14, 246–253. https://doi.org/10.1177/1479164117692766.
Oeckinghaus, A., Ghosh, S., 2009. The NF-κB family of transcription factors and its regulation. Cold Spring Harbor Perspect. Biol. 1, a000034. https://doi.org/10.1101/cshperspect.a000034.
Pal, R., Palmieri, M., Loehr, J.A., Li, S., Abo-Zahrah, R., Monroe, T.O., Thakur, P.B., Sardiello, M., Rodney, G.G., 2014. Src-dependent impairment of autophagy by oxidative stress in a mouse model of Duchenne muscular dystrophy. Nat. Commun. 5, 4425. https://doi.org/10.1038/ncomms5425.
Panza, E., Vellecco, V., Iannotti, F.A., Paris, D., Manzo, O.L., Smimmo, M., Mitilini, N., Boscaino, A., de Dominicis, G., Bucci, M., Di Lorenzo, A., Cirino, G., 2021. Duchenne's muscular dystrophy involves a defective transsulfuration pathway activity. Redox Biol. 45, 102040 https://doi.org/10.1016/j.redox.2021.102040.
Parsanathan, R., Jain, S.K., 2018. Hydrogen sulfide increases glutathione biosynthesis, and glucose uptake and utilization in C2C12 mouse myotubes. Free Radic. Res. 52, 288–303. https://doi.org/10.1080/10715762.2018.1431626.
Pietraszek-Gremplewicz, K., Kozakowska, M., Bronisz-Budzynska, I., Ciesla, M., Mucha, O., Podkalicka, P., Madej, M., Głowniak, U., Szade, K., Stepniewski, J., Jez, M., Andrysiak, K., Bukowska-Strakova, K., Kaminska, A., Kostera-Pruszczyk, A., Jozkowicz, A., Loboda, A., Dulak, J., 2018. Heme oxygenase-1 influences satellite cells and progression of Duchenne muscular dystrophy in mice. Antioxidants Redox Signal. 29, 128–148. https://doi.org/10.1089/ars.2017.7435.
Podkalicka, P., Mucha, O., Bronisz-Budzyńska, I., Kozakowska, M., Pietraszek-Gremplewicz, K., Cetnarowska, A., Głowniak-Kwitek, U., Bukowska-Strakova, K., Cieśla, M., Kulecka, M., Ostrowski, J., Mikuła, M., Potulska-Chromik, A., Kostera-Pruszczyk, A., Józkowicz, A., Łoboda, A., Dulak, J., 2020. Lack of miR-378 attenuates muscular dystrophy in mdx mice. JCI Insight 5, 135576. https://doi.org/10.1172/jci.insight.135576.
Podkalicka, P., Mucha, O., Dulak, J., Loboda, A., 2019. Targeting angiogenesis in Duchenne muscular dystrophy. Cell. Mol. Life Sci. 76, 1507–1528. https://doi.org/10.1007/s00018-019-03006-7.
Podkalicka, P., Mucha, O., Kaziród, K., Bronisz-Budzyńska, I., Ostrowska-Paton, S., Tomczyk, M., Andrysiak, K., Stępniewski, J., Dulak, J., Łoboda, A., 2021. Age-dependent dysregulation of muscle vasculature and blood flow recovery after hindlimb ischemia in the *mdx* model of Duchenne muscular dystrophy. Biomedicines 9, 481. https://doi.org/10.3390/biomedicines9050481.
Podkalicka, P., Myszka, M., Dulak, J., Łoboda, A., 2022. Molecular mechanisms of Duchenne muscular dystrophy and new therapeutic strategies. Postepy Biochem. 68, 109–122. https://doi.org/10.18388/pb.2021_428.
Rosenberg, A.S., Puig, M., Nagaraju, K., Hoffman, E.P., Villalta, S.A., Rao, V.A., Wakefield, L.M., Woodcock, J., 2015. Immune-mediated pathology in Duchenne muscular dystrophy. Sci. Transl. Med. 7 https://doi.org/10.1126/scitranslmed.aaa7322, 299rv4-299rv4.
Saclier, M., Ben Larbi, S., My Ly, H., Moulin, E., Mounier, R., Chazaud, B., Juban, G., 2021. Interplay between myofibers and pro-inflammatory macrophages controls muscle damage in mdx mice. J. Cell Sci. 134, jcs258429. https://doi.org/10.1242/jcs.258429.
Sandri, M., 2010. Autophagy in skeletal muscle. FEBS (Fed. Eur. Biochem. Soc.) Lett. 584, 1411–1416. https://doi.org/10.1016/j.febslet.2010.01.056.
Schäcke, H., Döcke, W.D., Asadullah, K., 2002. Mechanisms involved in the side effects of glucocorticoids. Pharmacol. Ther. 96, 23–43.
Shefa, U., Kim, M.-S., Jeong, N.Y., Jung, J., 2018. Antioxidant and cell-signaling functions of hydrogen sulfide in the central nervous system. Oxid. Med. Cell. Longev. 2018, e1873962 https://doi.org/10.1155/2018/1873962.
Sicinski, P., Geng, Y., Ryder-Cook, A.S., Barnard, E.A., Darlison, M.G., Barnard, P.J., 1989. The molecular basis of muscular dystrophy in the mdx mouse: a point mutation. Science 244, 1578–1580. https://doi.org/10.1126/science.2662404.
Tang, C., Li, X., Du, J., 2006. Hydrogen sulfide as a new endogenous gaseous transmitter in the cardiovascular system. Curr. Vasc. Pharmacol. 4, 17–22. https://doi.org/10.2174/157016106775203144.
Wang, J., Wu, D., Wang, H., 2019. Hydrogen sulfide plays an important protective role by influencing autophagy in diseases. Physiol. Res. 68, 335–345. https://doi.org/10.33549/physiolres.933996.
Wang, M.-J., Cai, W.-J., Li, N., Ding, Y.-J., Chen, Y., Zhu, Y.-C., 2010. The hydrogen sulfide donor NaHS promotes angiogenesis in a rat model of hind limb ischemia. Antioxidants Redox Signal. 12, 1065–1077. https://doi.org/10.1089/ars.2009.2945.

Wetzel, M.D., Wenke, J.C., 2019. Mechanisms by which hydrogen sulfide attenuates muscle function following ischemia–reperfusion injury: effects on Akt signaling, mitochondrial function, and apoptosis. J. Transl. Med. 17, 33. https://doi.org/10.1186/s12967-018-1753-7.

Wu, D., Hu, Q., Zhu, D., 2018. An update on hydrogen sulfide and nitric oxide interactions in the cardiovascular system. Oxid. Med. Cell. Longev. 1–16. https://doi.org/10.1155/2018/4579140, 2018.

Yu, Q., Lu, Z., Tao, L., Yang, L., Guo, Y., Yang, Y., Sun, X., Ding, Q., 2015. ROS-dependent neuroprotective effects of NaHS in ischemia brain injury involves the PARP/AIF pathway. Chem. Pharm. Bull. 36, 1539–1551. https://doi.org/10.1159/000430317.